PERGAMON

Journal of Structural Geology 23 (2001) 149–153

JOURNAL OF STRUCTURAL GEOLOGY

www.elsevier.nl/locate/jstrugeo

Ductile shear zones as counterflow boundaries in pseudoplastic fluids: Discussion and theory

Leslie J. Sonder

Department of Earth Sciences, Dartmouth College, 6105 Fairchild Hall, Hanover, NH 03755, USA

Received 24 March 2000; accepted 12 June 2000

Abstract

A model presented by Talbot (1999) attempts to use the shapes of S- or J-shaped structures in ductile shear zones experiencing simple shear to infer information about rock rheology, specifically the value of the stress exponent n in a power-law rheology. The model is incorrect, so cannot yield any insight into the deformation or rheology of shear zones. The shape of S- or J-shaped structures is more likely a function of variation across the shear zone of water fugacity, grain size, or other weakening mechanisms.

1. Introduction

Talbot (1999, hereafter referred to as Talbot) hypothesizes that the characteristic S- or J-shaped displacement patterns observed within ductile shear zones are a consequence of power law flow of material having differing stress exponents $n > 1$. However, his mathematical model is physically incorrect, and in fact variations in *n cannot* account for variations in S- and J-shaped displacement patterns. In this paper I discuss why Talbot's model is in error and why his hypothesis cannot explain observed displacement patterns in ductile shear zones undergoing simple shear. Instead, I suggest that weakening processes such as hydrolytic weakening or grain size reduction, if variable across a shear zone, can produce velocity profiles with S- or J-shapes like structures observed in shear zones.

2. Talbot's solution: shear zone deformation driven by an along-strike pressure gradient

Because the derivation is relevant to later discussion, I re-derive Talbot's expression. Let a shear zone of width w strike parallel to the x-direction and perpendicular to the y-direction (Fig. 1). Deformation in the third dimension (z-direction) is assumed constant and therefore is ignored. Channel flow in this shear zone is driven by a constant pressure gradient $\partial P/\partial x = -\Delta P/L$ parallel to the strike of the shear zone, where P is pressure and L is a characteristic along-strike length scale (e.g. Turcotte and Schubert 1982).

As Talbot notes, the only incompressible deformation that can occur in shear zones of constant width is simple shear. For the geometry shown in Fig. 1, this means that $\partial u/\partial y$ is the only non-zero velocity gradient and $\dot{\varepsilon}_{xy} = 1/2\ \partial u/\partial y$ is the only non-zero component of strain rate. Under these conditions the equations of motion reduce to the single equation

$$\frac{\partial \tau_{xy}}{\partial y} = \frac{\partial P}{\partial x}. \tag{1}$$

For a fluid deforming by power law creep, the strain rate $\dot{\varepsilon}_{xy}$ is related to deviatoric stress τ_{xy} by

$$\tau_{xy} = C^{-\frac{1}{n}} \dot{\varepsilon}_{xy}^{\frac{1}{n}} \tag{2}$$

where n is the stress exponent and C is a rheological parameter that can depend on factors such as temperature, fluid content, and grain size (e.g. see reviews by Evans and Dresen, 1991; Kohlstedt et al., 1995), but which in Talbot's analysis is taken as constant. Substituting for stress, strain rate, and pressure gradient in Eq. (1) gives

$$\frac{d\left[\left(\frac{du}{dy}\right)^{\frac{1}{n}}\right]}{dy} = -C^{\frac{1}{n}} \frac{\Delta P}{L}. \tag{3}$$

With no-slip boundary conditions, $u = 0$ on $y = \pm w/2$,

E-mail address: leslie.sonder@dartmouth.edu (L. Sonder).

0191-8141/01/$ - see front matter
PII: S0191-8141(00)00131-0

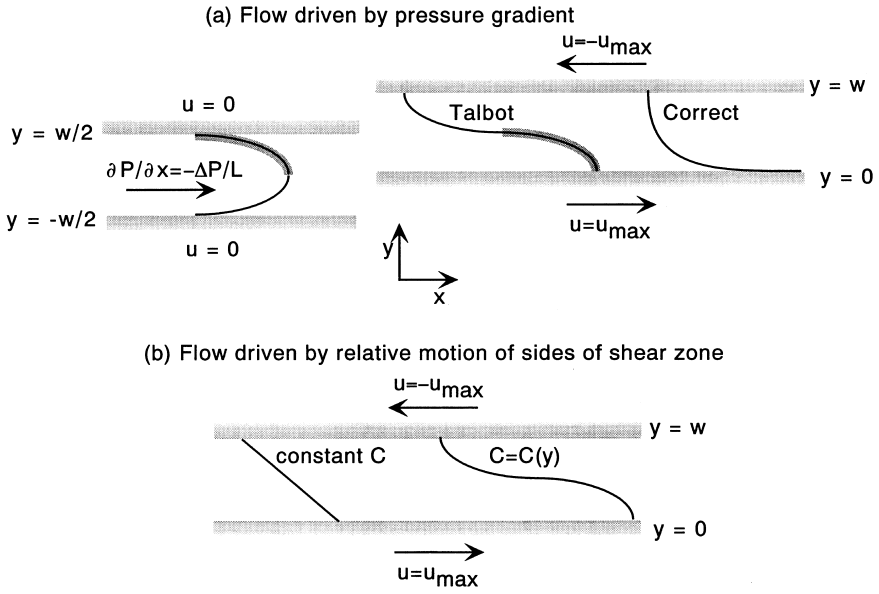

Fig. 1. (a) Geometry of original channel flow model (left-hand side) and Talbot's model (right-hand side), and sketches of resulting velocity distributions. In the original model (Turcotte and Schubert 1982), flow is driven by a pressure gradient and confined between fixed boundaries at $y = \pm w/2$. The velocity (or displacement) distribution is parabolic and symmetric about $y = 0$. Note that the entire solution can be constructed by taking half of the solution (from $0 = y = w/2$, shown with grey highlight) and joining it across $y = 0$ to its reflection. Talbot took this half of the solution, but joined it across $y = w/2$ to its inverse, constructing an antisymmetric function having apparent boundary conditions $u = u_{max}$ at $y = 0$ and $u = -u_{max}$ at $y = w$. The correct solution for these boundary conditions is shown at the far right of the figure and has no symmetry. (b) Geometry and boundary conditions for flow driven by relative motions of sides of shear zones. If the shear zone has constant width, there are no along-strike changes, and the rheological parameter C (Eq. (2)) is constant, the velocity distribution is linear regardless of the value of the stress exponent n. However, if C is spatially variable (e.g. due to variable fluid fugacity), the velocity distribution is nonlinear. The example illustrated here results from water fugacity increasing symmetrically and linearly from a minimum value at the boundaries to a maximum at the center of the shear zone.

the solution is

$$u = \frac{C}{n+1}\left(\frac{\Delta P}{L}\right)^n\left[\left(\frac{w}{2}\right)^{n+1} - \left|y\right|^{n+1}\right] \quad (4)$$

(Turcotte and Schubert, 1982, eq. 7-121) which when non-dimensionalized by the maximum velocity u_{max} (at y = 0) is

$$u/u_{max} = 1 - (2|y|/w)^{n+1}. \quad (5)$$

This solution is quoted by Talbot and is sketched on the left side of Fig. 1(a). It is symmetric across the solution

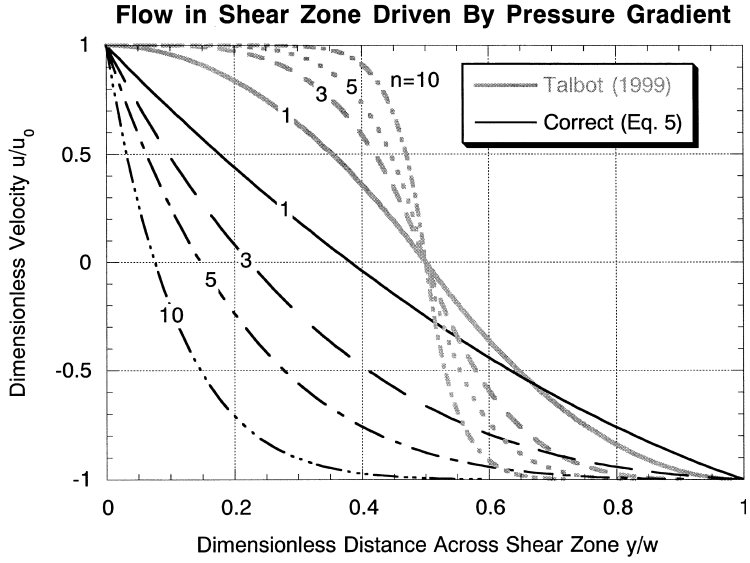

Fig. 2. Comparison of Talbot's solution (grey curves) with corrected solution (black curves) for flow in shear zone driven by a pressure gradient. Numbers on curves are values of the stress exponent n.

domain $-w/2 \leqslant y \leqslant w/2$. However, Talbot applied it to a different domain, from $0 \leqslant y \leqslant w$, ignoring the boundary at y = w/2, and instead implying apparent boundary conditions $u = +u_{max}$ at $y = 0$ and $u = -u_{max}$ at $y = w$. Doing so produces S-shaped curves, which are sketched in the middle of Fig. 1(a) and plotted for several values of n in Fig. 2.

Talbot's curves must be incorrect, as they are inconsistent with Eq. (3) which has the form $d/dy[(du/dy)^{1/n}] = \text{constant}$. Clearly for $n = 1$ this implies that the curvature (d^2u/dy^2) must be constant over the entire solution domain. When $n > 1$, the curvature is inversely proportional to $(du/dy)^{(1-1/n)}$, so as long as du/dy does not change sign, as it does not in Talbot's curves (Fig. 2), the curvature must have the same sign over the solution domain. Yet the curvatures of Talbot's solutions do change sign at $y = w/2$, for both $n = 1$ and $n > 1$.

Although demonstrated here in terms of violation of the requirements for the mathematical form of the velocity profile, the conclusion is identical to Fletcher's (this issue) based on the mechanical requirement for continuity of normal stress within the shear zone: Talbot's model is physically incorrect.

The physically correct solution for flow driven by a pressure gradient parallel to the shear zone and with Talbot's boundary conditions ($u = u_{max}$ at $y = 0$ and $u = -u_{max}$ at $y = w$) is actually

$$\frac{u}{u_{max}} = 1 - 2\frac{K_1^{n+1} - \left(K_1 - C^{1/n}\frac{\Delta P}{L}y\right)^{n+1}}{C^{1/n}\frac{\Delta P}{L}(n+1)u_{max}} \tag{6}$$

where $K_1 = u_{max}/w + C\Delta P/2$ when $n = 1$ and is expressed implicitly as

$$K_1^{n+1} = u_{max}C^{1/n}\frac{\Delta P}{w}(n+1) + \left(K_1 - C^{1/n}\Delta P\right)^{n+1} \tag{7}$$

when $n > 1$. This solution is also plotted in Fig. 2 and differs from Talbot's solution. Most obviously, it is not symmetric. Flow concentrates near one boundary and is suppressed on the other side where fluid is forced by the boundary condition to move from lower towards higher pressure.

Clearly, flow driven by a pressure gradient parallel to the strike of the shear zone cannot produce displacement or velocity profiles that match the observed S- or J-shaped strain markers. It is much more likely that flow in shear zones is a function of the relative velocities of the two sides of the shear zone. In the next section I explore such models.

3. Shear zone deformation due to relative motion of the sides

In the absence of a pressure gradient, the equation of motion for simple shear deformation states that shear stress is constant:

$$\frac{d\tau_{xy}}{dy} = 0. \tag{8}$$

Under the same assumptions as above (power-law rheology and boundary conditions $u = u_{max}$ at $y = 0$, $u = -u_{max}$ at $y = w$), it is straightforward to verify that the solution to Eq. (8) is

$$u = u_{max}\left(1 - \frac{2y}{w}\right). \tag{9}$$

Thus, regardless of the value of n, velocity varies linearly across the shear zone. Clearly, this model cannot account for the curved or sigmoidal pattern of displacements across shear zones.

The simplest circumstance allowing for formation of S-shaped velocity profiles is, instead, that the rheology varies across strike. Indeed, ductile shear zones are commonly thought to result from some sort of softening process (e.g. Davis and Reynolds, 1996).

Two common mechanisms for softening in materials deforming by dislocation creep or diffusion creep are hydrolytic weakening and grain size reduction. Rock mechanics experiments suggest that the deformation of quartz-rich materials undergoing power-law creep depends on a power m/n of the water fugacity f_{H2O}:

$$\tau = A^{-1/n}f_{H_2O}^{-m/n}e^{Q/nRT}\,\dot{\varepsilon}^{1/n} \tag{10}$$

where A is a pre-exponential constant, Q is the activation energy, R the gas constant, and T the absolute temperature. Experiments suggest that m/n is in the range 0.3–0.5 (Gleason and Tullis, 1995; Kohlstedt et al., 1995; Kronenberg and Tullis, 1984; Post et al., 1996), so for values of n appropriate for quartz, between 2 and 4 (Carter and Tsenn, 1987), m is probably between 1 and 2.

Alternatively, grain-size reduction (e.g. due to progressive deformation) weakens materials undergoing diffusion (linear) creep according to:

$$\tau = A^{-1}d^he^{Q/RT}\,\dot{\varepsilon} \tag{11}$$

where the exponent h is 2 or 3 (Turcotte and Schubert, 1982).

Both rheologies can be expressed by Eq. (2) if C, which includes variable water fugacity, grain size, temperature, or other environmental parameters, is considered variable. If so, then integrating the equation of motion (8) gives

$$u = K_1\int C(y)dy + K_2 \tag{12}$$

where K_1 and K_2 are constants of integration.

A more explicit solution requires specifying how C varies with position, which in turn requires specifying how water fugacity or grain size varies with position. To illustrate, consider variable water fugacity, $f_{H20.}$ Assume that f_{H20} increases linearly across half of the shear zone, from f_0 at the edge $y = 0$ of the shear zone to f_1 at the center $y = w/2$,

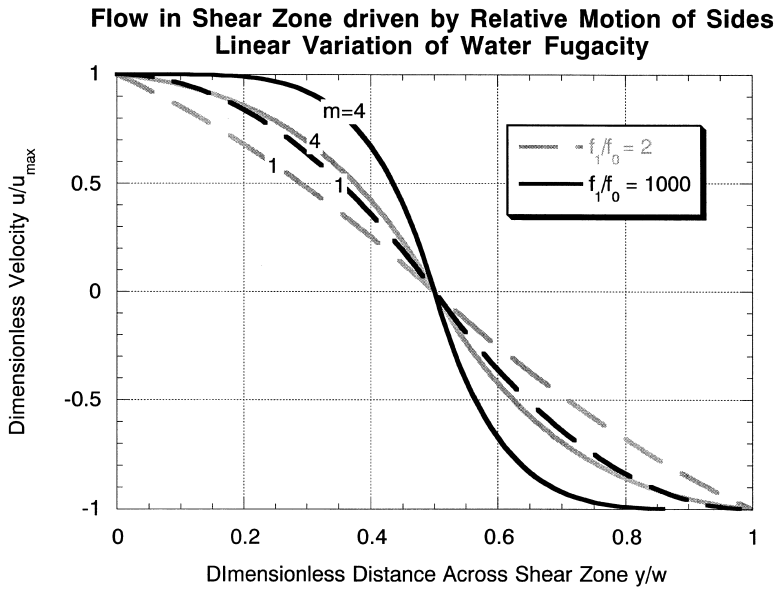

Fig. 3. Velocity and shear stress distribution for flow in a shear zone driven by relative motion of its sides, when water fugacity increases linearly and symmetrically from f_0 at the sides to f_1 at the center. Grey curves are for small variation in water fugacity ($f_1/f_0 = 2$) and black curves are for large variation in water fugacity ($f_1/f_2 = 10^3$). When $f_1/f_0 >> 1$, the shape of these curves identically matches that of Talbot's (Fig. 2).

and symmetrically decreases across the other half of the shear zone. (The resulting solution also applies to the mathematically equivalent scenario in which grain size h decreases inversely with y, as long as $h = m/n$.)

The oxygen fugacity is

$$f_{H_2O} = \begin{matrix} f_0 + 2(f_1 - f_0)y/w \\ f_0 + 2(f_1 - f_0)(1 - y/w) \end{matrix} \begin{cases} 0 \le y \le w/2 \\ w/2 \le y \le w \end{cases} \tag{13}$$

Substituting for water fugacity in Eq. (12) using Eqs. (13) and (10) and using the same boundary conditions as before yields the velocity distribution in a shear zone with linearly varying water fugacity:

$$\frac{u}{u_{\max}} = \begin{matrix} \dfrac{\left(\dfrac{f_0 + 2(f_1 - f_0)y/w}{f_1}\right)^{1+m} - 1}{\left(\dfrac{f_0}{f_1}\right)^{1+m} - 1} \\ \dfrac{\left(\dfrac{f_0 + 2(f_1 - f_0)(1 - y/w)}{f_1}\right)^{1+m} - 1}{\left(\dfrac{f_0}{f_1}\right)^{1+m} - 1} \end{matrix} \begin{cases} 0 \le y \le w/2 \\ w/2 \le y \le w \end{cases} . \tag{14}$$

Plots of this solution (Fig. 3) show S-shaped curves similar to Talbot's curves. In fact, inspection of Eqs. (4) and (14) shows that if $f_1 >> f_0$ and $m = n$, the mathematical form is identical. Like Talbot's curves, a change in curvature occurs at $y = w/2$; however the change in curvature is consistent with the equation of motion when variable rheology is incorporated and is thus physically plausible.

4. Comparison of simple models with the examples provided by Talbot

The examples given by Talbot in his figs. 9–12 provide an interesting array of deformed structures in a variety of environments and over a wide range of scales. They also provide a reminder of the care that must be taken when applying models to real examples, since several (e.g. Talbot's figs. 11(a) and 11(c), the Mancos Shale–Mesaverde Sandstone contact in the San Juan Basin of Colorado (USA) and the Alpine fault in New Zealand) appear to violate model assumptions that deformation is constant along strike of the shear zone. These examples are thus not relevant to Talbot's attempted analysis.

The bent structures near the East Pacific rise shown by Talbot in his fig. 10(b) require a different explanation altogether. They have curvature *opposite* in sense to the displacement on the adjacent left-lateral transform faults, so cannot be formed by simple shear along the transform. Instead, they are examples of so-called J-structures (e.g. Crane, 1976; Fox and Gallo, 1984) formed near ridge-transform intersections and generally thought to be extensional fractures forming along mid-ocean ridges. These fractures change orientation with proximity to the ridge-transform intersection due to a greater contribution to the net stress field from shear stresses along the transform (Fox and Gallo, 1984; Fujita and Sleep, 1978; Lonsdale, 1978; Phipps Morgan and Parmentier, 1984; Searle, 1984).

The other examples given by Talbot in his figs. 10–12 are ductile shear zones having displacement profiles for which his incorrect analysis suggests $n = 5$. They are better explained by a model in which deformation results from the relative motions of the sides of a zone within which

increased fluid fugacity, grain size reduction, or some other mechanism has weakened the rock. All the examples that Talbot fit with $n = 3$ can be directly fitted with such models, which have m or $h = 3$. Examples fit by Talbot with n between 3 and 5 have curvatures more extreme than can be obtained from Eq. (14) if water fugacity varies linearly. They could be fit by adopting a nonlinear variation of water fugacity, but since it is difficult to independently constrain the distribution of fluid fugacity, little is to be gained by such an exercise. The object here is not to attempt to uniquely determine the distribution of fluid fugacity, but to suggest that geologically reasonable spatial variations in fluid fugacity or grain size can, in general, produce S-shaped velocity profiles. If such profiles, generated from temporally constant velocity fields, approximate the formation over time of displacement profiles in field examples, then these models may be useful guides towards better understanding of the links between weakening mechanisms, such as grain size reduction or hydrolytic weakening, and the strain and displacement distribution within shear zones.

5. Conclusions

From simple models of deformation in shear zones, Talbot (1999) proposes that the shapes of J- or S-shaped structures observed in many shear zones directly reflect the value of the stress exponent n in the power-law rheology governing flow. However, his model violates physical law. Although I agree with Talbot that such structures offer clues to the dynamics of deformation in shear zones, I suggest that their shapes depend on variable fluid fugacity, grain size, or other mechanisms that weaken the rock and localize deformation. A model incorporating this hypothesis produces velocity profiles that match structures in observed shear zones equally as well as Talbot's, but without violating physical principles.

Acknowledgements

The arguments in this paper were originally made in a letter to Chris Talbot, who acted with commendable scientific integrity by suggesting that I publish them. Thanks to the editor of the Journal of Structural Geology for his help, to Kelsey Sinclair and Anthony Faiia for their comments on an early version of this paper, and to Ray Fletcher for his review.

References

Carter, N.L., Tsenn, M.C., 1987. Flow properties of continental lithosphere. Tectonophysics 136, 27–63.

Crane, K., 1976. The intersection of the Siqueiros transform fault and the East Pacific Rise. Marine Geology 21, 25–46.

Davis, G.H., Reynolds, S.J., 1996. Structural Geology of Rocks and Regions. John Wiley & Sons, New York.

Evans, B., Dresen, G., 1991. Deformation of Earth materials: Six easy pieces. Review of Geophysics supplement, 823–843.

Fox, P.J., Gallo, D.G., 1984. A tectonic model for ridge-transform-ridge plate boundaries: Implications for the structure of oceanic lithosphere. Tectonophysics 104, 205–242.

Fujita, K., Sleep, N.H., 1978. Membrane stresses near mid-ocean ridge-transform intersections. Tectonophysics 50, 207–221.

Gleason, G.C., Tullis, J., 1995. A flow law for dislocation creep of quartz aggregates determined with the molten salt cell. Tectonophysics 247, 1–23.

Kohlstedt, D.L., Evans, B., Mackwell, S.J., 1995. Strength of the lithosphere: Constraints imposed by laboratory experiments. Journal of Geophysical Research 100, 17587–17602.

Kronenberg, A.K., Tullis, J., 1984. Flow strengths of quartz aggregates: Grain size and pressure effects due to hydrolytic weakening. Journal of Geophysical Research 89, 4281–4297.

Lonsdale, P., 1978. Near-bottom reconnaissance of a fast-slipping transform fault zone at the Pacific-Nazca plate boundary. Journal of Geology 86, 451–472.

Phipps Morgan, J., Parmentier, E.M., 1984. Lithospheric stress near a ridge-transform intersection. Geophysical Research Letters 11, 113–116.

Post, A.D., Tullis, J., Yund, R.A., 1996. Effects of chemical environment on dislocation creep of quartzite. Journal of Geophysical Research 101, 22143–22155.

Searle, R., 1984. GLORIA survey of the East Pacific Rise Near 3.5°S: Tectonic and volcanic characteristics of a fast spreading mid-ocean rise. Tectonophysics 101, 319–344.

Talbot, C.J., 1999. Ductile shear zones as counterflow boundaries in pseudoplastic fluids. Journal of Structural Geology 21, 1535–1551.

Turcotte, D.L., Schubert, G., 1982. Geodynamics. Wiley, New York.